

Tunable transmission and bistability in left-handed bandgap structures

Michael W. Feise, Ilya V. Shadrivov, and Yuri S. Kivshar

*Nonlinear Physics Centre, Centre for Ultra-high bandwidth Devices for Optical Systems (CUDOS),
Research School of Physical Sciences and Engineering,
Australian National University, Canberra, ACT 0200, Australia*

(Dated: September 3, 2018)

We study the defect-induced nonlinear transmission of a periodic structure created by alternating slabs of two materials with positive and negative refractive index. We demonstrate bistable switching and tunable nonlinear transmission in a novel type of bandgap that corresponds to the vanishing average refractive index, and compare the observed effects for two types of the bandgaps.

Materials with both negative electric permittivity and negative magnetic permeability were suggested theoretically a long time ago [1] and they were termed *left-handed materials* [2]. Such materials can also be described by a negative refractive index, as was demonstrated by several reliable experiments [3, 4] and numerical finite-difference time-domain simulations [5].

Multilayered structures composed of left-handed (LH) materials can be considered as a sequence of flat lenses that provide an optical cancellation of the conventional right-handed (RH) layers leading to either enhanced or suppressed transmission [6, 7]. More importantly, a one-dimensional stack of layers with alternating RH and LH material with vanishing average refractive index $\langle n \rangle$ displays a novel bandgap [8, 9, 10] that differs from a conventional Bragg reflection gap.

In this letter, we study defect-induced bistable switching in the novel bandgap structures and, for the first time to our knowledge, compare the effects observed for zero-index and Bragg reflection gaps. The particular structure we study by numerical pseudospectral time-domain (PSTD) simulations consists of seven periods of a LH-RH double-layer (indicated in Fig. 1). Each individual layer has equal width a . The LH layer of the central period is replaced by a Kerr-type nonlinear material, which constitutes a structural defect of the periodic system even in the linear regime. We also study the effects produced by a change of the defect position for two types of bandgaps.

We calculate the electric and magnetic fields directly from Maxwell's equations using the PSTD method [11]. The differential Maxwell equations are approximated by difference equations and solved iteratively. The material properties are treated through the electric permittivity ε_r and magnetic permeability μ_r . The PSTD method is advantageous for the modeling of interfaces where both ε_r and μ_r change because it samples all material properties at the same location [12].

The linear properties of the LH material are described by Lorentz dispersion characteristics in both ε_r and μ_r ,

$$\varepsilon_r(\omega) = 1 + \frac{\omega_{pe}^2}{\omega_{1e}^2 - \omega^2 - i\gamma_e\omega}, \quad (1)$$

$$\mu_r(\omega) = 1 + \frac{\omega_{pm}^2}{\omega_{1m}^2 - \omega^2 - i\gamma_m\omega}. \quad (2)$$

These functions are substituted into the relations,

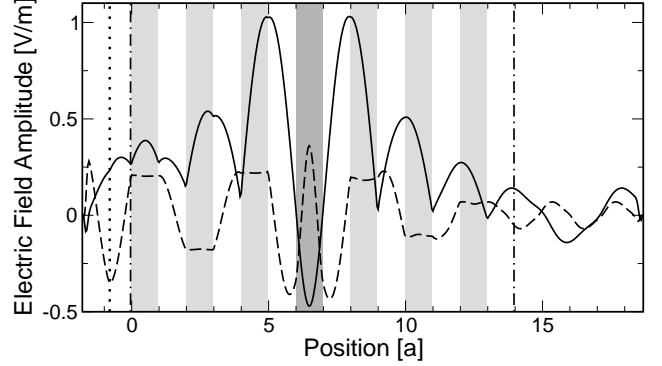


FIG. 1: Layout of the system with snapshots of the electric field amplitude. A Gaussian pulse with carrier frequencies $\omega_c = 2\pi \times 14.93$ GHz (solid) and $\omega_c = 2\pi \times 25.88$ GHz (dashed) is incident on the structure. The fields are shown at the pulse peak. The shaded background indicates the material structure, with dark grey denoting the Kerr material and light grey the LH slabs. The defect layer is centered within the structure. The dotted vertical line shows the source location, the dash-dotted vertical lines denote the boundaries of the considered structure. The field is incident from the left.

$\mathbf{D}(\omega) = \varepsilon_r(\omega)\varepsilon_0\mathbf{E}(\omega)$, $\mathbf{B}(\omega) = \mu_r(\omega)\mu_0\mathbf{H}(\omega)$, transformed into ordinary differential equations in the time domain, and subsequently approximated by difference equations [13] that are incorporated into the PSTD algorithm. This allows one to model frequency dependent material properties in PSTD simulations. The nonlinear Kerr material is described by a dielectric function

$$\varepsilon_r^{\text{NL}} = 1 + \chi^{(1)} + \chi^{(3)} |\mathbf{E}(t)|^2. \quad (3)$$

There are several established methods of including the nonlinear material response in the PSTD algorithm [14, 15, 16, 17]. Here, we use the electric field of the previous time step to evaluate Eq. (3) [15, 16].

We also calculate the properties of the structure using the transfer-matrix method (TMM) [18]. This method allows an exact analytical solution of the linear problem. In particular, one can relate incident, transmitted and reflected fields using the transfer matrix of the structure, and thus obtain an explicit expression for the transmission and reflection coefficients.

We describe the LH material by Eqs. (1),(2) with parameters chosen to give a refractive index $n \approx -1$ at

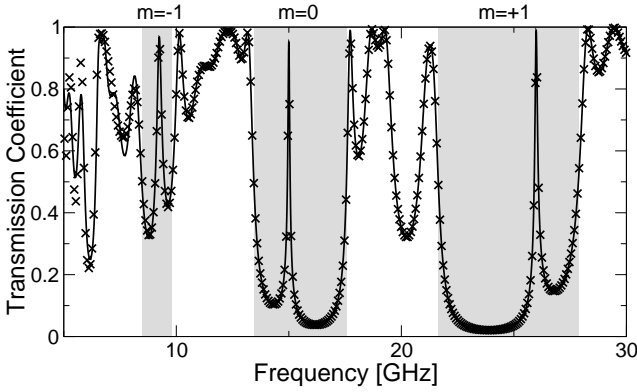


FIG. 2: Linear amplitude transmission coefficient of the structure calculated by the TMM (line) and PSTD (symbols) methods. The band gaps are indicated by shaded regions. The $\langle n \rangle = 0$ ($m = 0$) bandgap lies around 15 GHz. The first conventional Bragg gap ($m = +1$) lies around 25 GHz while the first Bragg gap in the left-handed regime ($m = -1$) lies around 9 GHz.

the design frequency $f_0 = 15$ GHz. We use $\omega_{pe} = 1.1543 \times 10^{11} \text{ s}^{-1}$, $\omega_{1e} = \omega_{1m} = 2\pi \times 5 \times 10^6 \text{ s}^{-1}$, and $\omega_{pm} = 1.6324 \times 10^{11} \text{ s}^{-1}$, and include small losses, $\gamma_e = 2 \times \gamma_m = 2\pi \times 6 \times 10^6 \text{ s}^{-1}$. With these parameters the LH meta-material is left-handed for frequencies $f < 18.5$ GHz and right-handed for $f > 26$ GHz. The slab thickness a is chosen to be $\lambda_0/4$, where λ_0 is the free-space wavelength at f_0 . We use air as the RH medium. The parameters for the Kerr material are $\chi^{(1)} = 3$ and $\chi^{(3)} = 4 \text{ m}^2/\text{V}^2$. In each case the PSTD simulations use a discretization of 100 points per λ_0 and a time step corresponding to half the Courant stability limit [11] of the linear case.

To validate our PSTD calculations, we first study the amplitude transmission spectrum in the linear regime, shown in Fig. 2, and find excellent agreement between the TMM and PSTD methods. For frequencies below 8 GHz, the discretization level in the PSTD simulations is insufficient for accurate results, due to the high refractive index of the LH material, and some discrepancies appear. The structure exhibits band gaps due to Bragg scattering, both in the RH and in the LH frequency region. An additional band gap appears around the frequency where the average refractive index vanishes, as was addressed earlier [8, 9, 10]. These band gaps can be identified through the index m in the usual Bragg condition,

$$k_{RH}a_{RH} + k_{LH}a_{LH} = m\pi, \quad (4)$$

where k_j is the respective wave number and a_j is the respective layer thickness. The band gap index m can be any integer, including zero and negative numbers. We find that the defect layer introduces a transmission peak into each of the shown band gaps. The remainder of this letter will focus on the comparison of the $\langle n \rangle = 0$ gap ($m = 0$) and the first RH Bragg gap ($m = +1$).

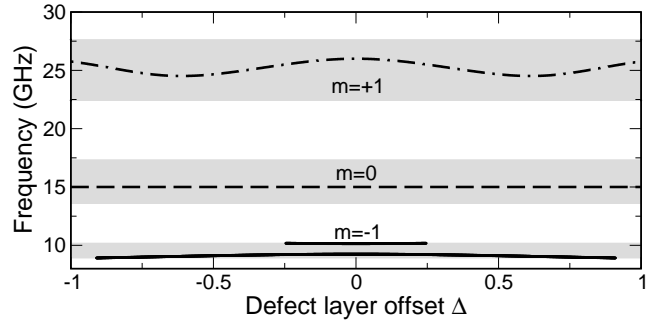


FIG. 3: Dependence of the defect frequency on the position offset Δ of the defect layer in the linear limit.

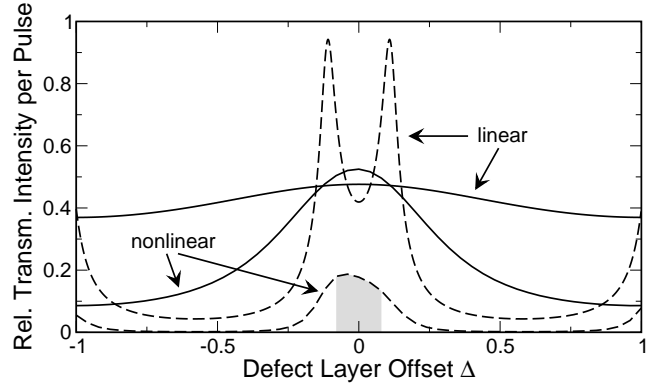


FIG. 4: Time-integrated transmitted intensity per pulse, relative to that of the incident pulse, in the $m = 0$ gap (solid) and the $m = +1$ gap (dashed). Bistability occurs in the $m = 0$ gap for all offsets, while the bistability region for the $m = +1$ gap is indicated in the graph by grey shading.

We calculate the frequency of the defect modes in the band gaps for different locations of the defect layer in our structure in the linear case, as shown in Fig. 3. The defect layer is shifted by a quantity $a\Delta$ ($|\Delta| \leq 1$) from the central position ($\Delta = 0$) between its two neighboring LH layers without changing the rest of the structure. It is remarkable that in the $m = 0$ gap the defect frequency *does not depend on the defect position* while the one in the $m = +1$ gap is shifted with changing Δ . When the thickness of the defect layer is not equal to a (not shown), the $m = 0$ defect frequency also depends on Δ . This dependence, however, is much weaker than that of the $m = +1$ defect.

In the nonlinear regime, the behavior of the fields depends on the intensity of the electric field inside the nonlinear layer. We study this problem by PSTD simulations. The incident field has a Gaussian envelope in time with a width parameter of $1528/f_0$ and amplitude 0.2 V/m . The carrier frequency is $\omega_c = 2\pi \times 14.93 \text{ GHz}$ for the $m = 0$ band gap and $\omega_c = 2\pi \times 25.88 \text{ GHz}$ for the $m = +1$ gap. These frequencies lie below their respective defect frequencies at $\Delta = 0$ with equal relative detuning.

In Fig. 4 we show the relative time-integrated transmitted intensity per pulse versus the position of the non-

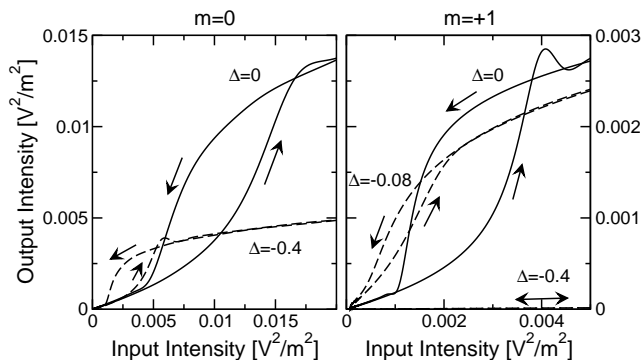


FIG. 5: Output vs. input intensity of the structure, showing hysteresis behavior for defect offsets of $\Delta = 0, -0.4$ in the $m = 0$ gap and $\Delta = 0, -0.08, -0.4$ in the $m = +1$ gap. The $\Delta = -0.4$ curve in the $m = +1$ gap is an almost vanishing straight line without bistability.

linear layer in the *linear* and *nonlinear* regimes for pulses at both carrier frequencies. The two bands display very different character. In the linear regime, the transmission in the $m = 0$ gap is only weakly dependent on Δ with a maximum at $\Delta = 0$. In the $m = +1$ gap, the linear transmission shows a double peak structure near $\Delta = 0$. Away from this region the transmission is much reduced. For $\Delta \approx \pm 1$ the transmission increases again. In the nonlinear case the transmission is generally reduced. In the $m = 0$ gap, it maintains its character with a single peak in the center, which actually exceeds the peak of the linear case. In the $m = +1$ gap, the double peak character is lost and a much smaller single peak in the center and weak wings for large layer offsets remain. For all other Δ the transmission almost vanishes.

One of the most promising applications of periodic structures with embedded nonlinear defect layers is the possibility to achieve intensity-dependent tunable trans-

mission in the spectral bandgaps usually associated with bistability. Optical bistability is a powerful concept that could be explored to implement all-optical logic devices and switches. In nonlinear systems that display bistability, the output intensity is a strong nonlinear function of the input intensity [19, 20].

In the $m = 0$ gap, we observe bistability for all offsets while in the $m = +1$ gap, bistability is observed for very small values of $|\Delta|$. These effects are related to the behavior of the defect frequency in the $m = +1$ gap with different Δ . In this gap the defect frequency shifts away from the carrier frequency with increased Δ and eventually approaches it again. In contrast to this, the defect frequency in the $m = 0$ gap stays very near to the carrier frequency for all layer offsets. In Fig. 5 we show the output vs. input intensity during the time of the pulse. The left panel shows the behavior in the $m = 0$ gap for offsets $\Delta = 0$ and $\Delta = -0.4$, while the right panel shows the behavior in the $m = +1$ gap for offsets $\Delta = 0$, $\Delta = -0.08$, and $\Delta = -0.4$. The bistable behavior, where the output intensity with increasing input intensity is different from the one with decreasing input intensity, is clearly visible. The threshold switching intensity in the $m = +1$ gap is significantly lower than in the $m = 0$ gap. On the other hand, the difference between switch-up and switch-down threshold is much larger in the $m = 0$ gap. The difference between the behavior in the two gaps is illustrated by the $\Delta = -0.4$ curves. While the $m = 0$ gap shows significant bistability, the $m = +1$ gap shows no bistability and almost no transmission.

In conclusion, we have studied the defect-induced nonlinear transmission and bistability for two types of bandgaps of a layered structure composed of two materials with positive and negative refractive index with a Kerr nonlinear defect. We demonstrated a number of unique features of the bandgap associated with zero average refractive index of the structure.

-
- [1] V. G. Veselago, Sov. Phys. Usp. **10**, 509 (1968).
 - [2] J. B. Pendry, Opt. Express **11**, 639 (2003).
 - [3] R. A. Shelby, D. R. Smith, and S. Schultz, Science **292**, 77 (2001).
 - [4] R. B. Gregor, C. G. Parazzoli, K. Li, B. E. C. Koltenbah, and M. Tanielian, Opt. Express **11**, 688 (2003).
 - [5] S. Foteinopoulou, E. N. Economou, and C. M. Soukoulis, Phys. Rev. Lett. **90**, 107402 (2003).
 - [6] J. B. Pendry and S. A. Ramakrishna, J. Phys. Condens. Matter **15**, 6345 (2003).
 - [7] Z. M. Zhang and C. J. Fu, Appl. Phys. Lett. **80**, 1097 (2001).
 - [8] J. Li, L. Zhou, C. T. Chan, and P. Sheng, Phys. Rev. Lett. **90**, 083901 (2003).
 - [9] I. V. Shadrivov, A. A. Sukhorukov, and Y. S. Kivshar, Appl. Phys. Lett. **82**, 3820 (2003).
 - [10] L. Wu, S. He, and L. Shen, Phys. Rev. B **67**, 235103 (2003).
 - [11] Q. H. Liu, Microwave Opt. Technol. Lett. **15**, 158 (1997).
 - [12] M. W. Feise, J. B. Schneider, and P. J. Bevelacqua, arXiv:cond-mat/0401319, (2004).
 - [13] C. Hulse and A. Knoesen, J. Opt. Soc. Am. A **11**, 1802 (1994).
 - [14] P. M. Goorjian and A. Taflove, Opt. Lett. **17**, 180 (1992).
 - [15] R. W. Ziolkowski, IEEE Trans. Antennas Propagat. **45**, 375 (1997).
 - [16] C. Lixue, D. Xiaoxu, D. Weiqiang, C. Kiangcai, and L. Shutian, Opt. Commun. **209**, 491 (2002).
 - [17] P. Tran, Opt. Lett. **21**, 1138 (1996).
 - [18] P. Yeh, *Optical Waves in Layered Media* (John Wiley & Sons, New York, 1988).
 - [19] S. F. Mingaleev and Y. S. Kivshar, J. Opt. Soc. Am. B **19**, 2241 (2002).
 - [20] M. F. Yanik, S. H. Fan, and M. Soljacic, Appl. Phys. Lett. **83**, 2739 (2003).